

Organic & Biomolecular Chemistry

Accepted Manuscript



This is an *Accepted Manuscript*, which has been through the Royal Society of Chemistry peer review process and has been accepted for publication.

Accepted Manuscripts are published online shortly after acceptance, before technical editing, formatting and proof reading. Using this free service, authors can make their results available to the community, in citable form, before we publish the edited article. We will replace this *Accepted Manuscript* with the edited and formatted *Advance Article* as soon as it is available.

You can find more information about *Accepted Manuscripts* in the [Information for Authors](#).

Please note that technical editing may introduce minor changes to the text and/or graphics, which may alter content. The journal's standard [Terms & Conditions](#) and the [Ethical guidelines](#) still apply. In no event shall the Royal Society of Chemistry be held responsible for any errors or omissions in this *Accepted Manuscript* or any consequences arising from the use of any information it contains.

ARTICLE

Kinetics of reactions at interface: Functionalisation of silicate glass with porphyrins via covalent bonds

Cite this: DOI: 10.1039/x0xx00000x

Takahiro Fujimoto,^a Nao Furuta,^a and Tadashi Mizutani^{*a}Received 00th January 2012,
Accepted 00th January 2012

DOI: 10.1039/x0xx00000x

www.rsc.org/

Porphyrins carrying either a primary alcohol, tertiary alcohol or primary bromide linker group were allowed to react with the surface silanol groups on silicate glass thermally at 80–240 °C to obtain the monolayer film. Kinetics of the reaction was analysed based on the pseudo-second order equation. Tertiary alcohol and primary bromide reacted much slower than primary alcohol. Kinetics of the reaction was analysed by the pseudo-second order equation. Arrhenius plots indicated that higher activation energies can account for the slower reaction of both tertiary alcohol and primary bromide linkers. Introduction of six dodecyl chains to hydroxyporphyrin accelerated the anchoring reaction by a factor of 50 owing to the larger frequency factor of the reaction, demonstrating that the dynamics of the interface is one of the dominant factors regulating the reaction kinetics.

Introduction

Interface between metals or metal oxides and organic molecules¹ plays a crucial role in the functions of materials such as organic electronic devices and organic-inorganic hybrid mechanical materials.² For preparation of catalyst,³ adsorbent,⁴ and sensors⁵ loaded on silica, mesoporous silica or colloidal metal oxides, construction of interface between the functional molecule and inorganic surface is important. Therefore, the process of the preparation of desired interface structures and durability of such interfaces attracts interests of chemists as well as materials scientists. As a representative example of interface, self-assembled monolayer film on a substrate has been studied extensively.⁶

Porphyrins have unique optical and redox properties and are semiconductive in an assembled state, and its thin film formation on solid surfaces attracted great interest for possible applications in electronic and optical devices, catalyst, and adsorbent.⁷ We investigated the reaction of silicate glass with porphyrins bearing OH group(s) as an anchoring group(s) to attach it to silica surface. Owing to the large optical absorption coefficient of the porphyrin Soret band, even monolayer film of porphyrin on glass substrate can be quantitatively detected using transmission UV–visible spectroscopy. Therefore, kinetic study of the anchoring reaction and the hydrolysis reaction of the silicate ester bond on silicate glass were performed with high sensitivity and good reproducibility using UV–visible spectroscopy. The reaction of gaseous simple alcohols with silica has been studied since 1960s.⁸ It is noted that the reaction between porphyrins and silicate glass occurred at the interface between two solid phases, because the melting points of porphyrins were higher than the reaction temperature. Inhomogeneous nature of the solid surface led to the difficulty in kinetic analysis, and the reproducibility of the kinetic

experiments is sometimes poor. Owing to these issues, kinetic study of the anchoring reaction of organic molecules to solid surface has been rarely done. The reactivity of the organic reagent in the reaction across the interface should depend on the intrinsic reactivity of the molecule, the structure of the interface, and the dynamics of the interface where the reaction proceeds.

Previously, we reported that porphyrins with primary or tertiary alcohol group(s) were bound to silicate glass thermally via a solid-solid reaction, and kinetics of hydrolysis of the resulting monolayer film of porphyrin was studied.^{9,10} The major conclusions were (1) the rate of hydrolysis of primary alcohol-tethered and tertiary alcohol-tethered monolayer were similar under acidic conditions, while the rate of latter monolayer was much slower than the rate of the former monolayer under alkaline conditions, (2) isotope labelling studies showed that there is a covalent bond between the porphyrin and silicate glass, and (3) the C-O bond of the tertiary alcohol tethered silicate glass was cleaved under acidic conditions.

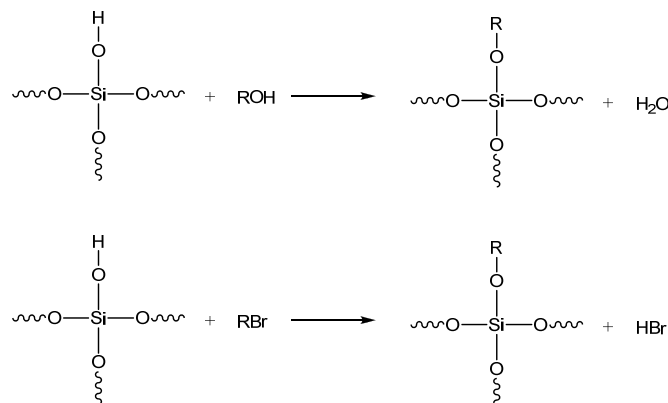
In this paper, we focus on factors of controlling the kinetics of the anchoring reaction of porphyrins bearing either hydroxyl or bromo group(s) to silicate glass, with particular attention to the relative contribution of the intrinsic reactivity of the functional group and the dynamics of interface. While hydrolysis of monolayer occurs at the solid-liquid interface, the anchoring reaction occurs at the solid-solid interface, and the kinetics was complicated. The rate of the anchoring reaction was analysed based on the pseudo-second order equation. Based on the pseudo-second order rate constants, activation energies and frequency factors were determined. We found that introduction of dodecyl chains to hydroxyporphyrin accelerated the anchoring reaction by a factor of 50, and this acceleration was ascribed to the larger frequency factor of the reaction. These findings should shed light on the mechanism of the reactions at the interface, and lead to rational design of the anchoring reactions.

Results and Discussion

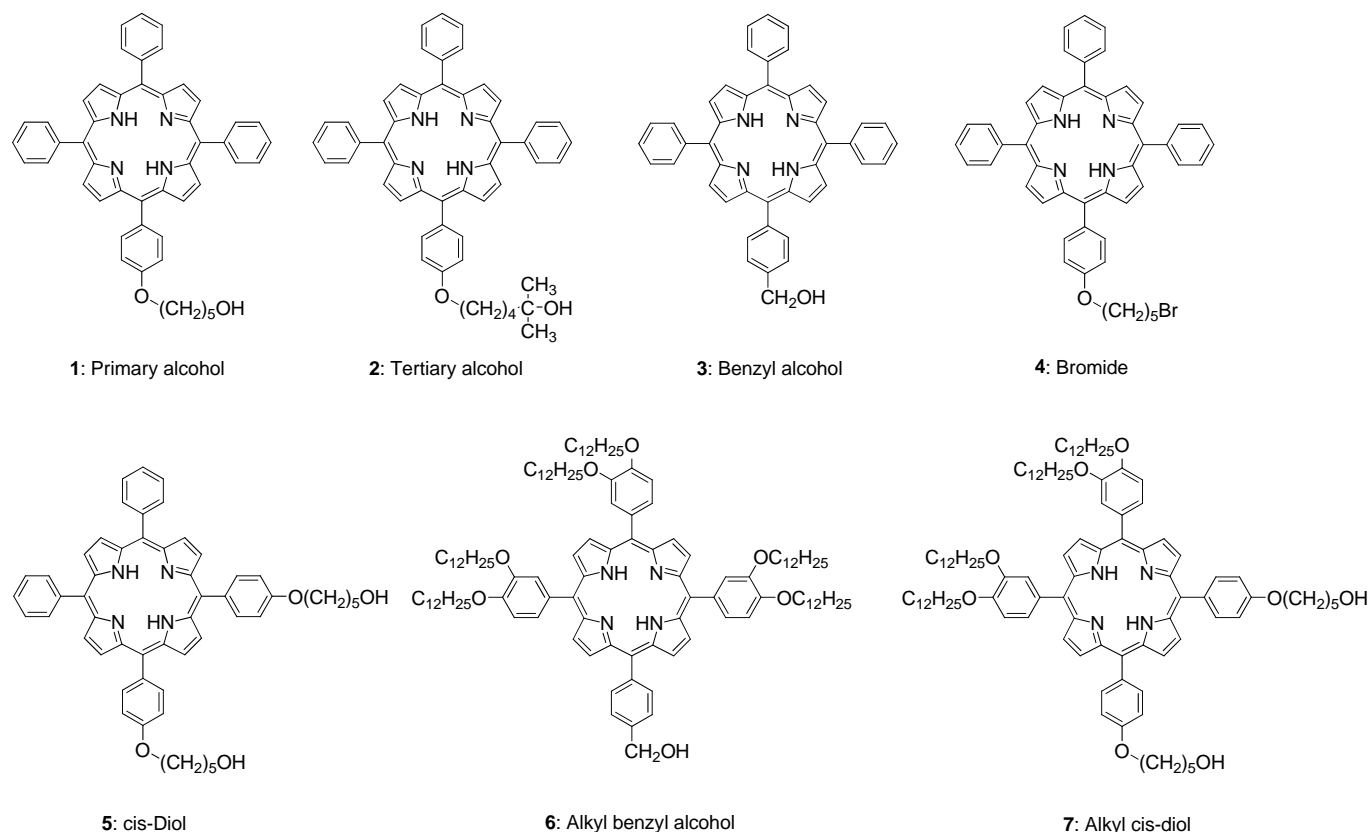
Porphyrins with various anchoring groups

We investigated the reactions of seven porphyrins having either a hydroxy or bromo group as an anchoring group with silicate glass (Scheme 1). The structures of the porphyrins are shown in Scheme 2. Porphyrins **1** and **2** have a primary alcohol or tertiary alcohol linker connected through a flexible pentamethylene spacer, respectively. Porphyrin **3**¹¹ has a primary alcohol linker with a shorter methylene spacer. Porphyrin **4**¹² has a primary bromoalkyl linker. Porphyrin **5** has a divergent diol linker. Porphyrins **6** and **7** have long alkyl chains, which could facilitate the molecular reorientation during the reaction to aid the access of the hydroxy group to the silanol group on the silicate glass. The melting points of these porphyrins were 284 °C (**1**), 259 °C (**2**), >300 °C (dec) (**3**), 278 °C (**4**), 271 °C (**5**), 120 °C (**6**), and 135 °C (**7**). Porphyrins with OH group(s) or a Br atom without alky chains have high melting points. For porphyrins **1–7**, typical reaction temperatures were 80–240 °C, lower than the melting points, and the reaction occurred at the solid-solid interface. Owing to the high melting points of these porphyrins, molecular motion is an influencing factor of the kinetics of the reaction.

Alkyl porphyrins **6** and **7** showed much lower melting points, and the reaction temperature is comparable to the melting points. The reaction of **6** and **7** with silicate glass occurred at the liquid-solid interface when the heating temperature was higher than the melting points.



Scheme 1 Reactions of alcohols and bromides with silicate glass.



Scheme 2 Porphyrins with various linker groups.

UV-visible spectroscopic studies of reactions of porphyrins with silicate glass

A spin coated film of porphyrins on silicate glass was heated on a hot stage, and the UV-visible spectrum of the glass was

recorded after the silicate glass was washed with toluene to remove the unreacted porphyrin. A representative example of the spectral changes for the reaction of **1** with silicate glass is shown in Figure 1. As heating was continued, the absorbance of the Soret band increased with a slight red shift. The UV-visible spectrum of **1** in toluene exhibited the absorption maximum of

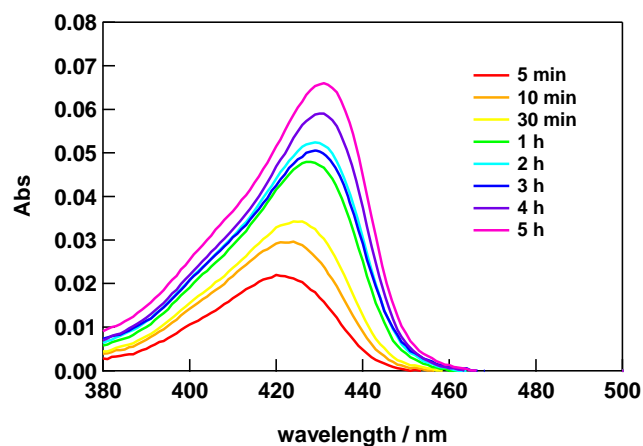


Fig. 1 UV-visible spectral changes of spin coated film of primary alcohol porphyrin 1 on silicate glass after heated at 140 °C and rinsed with toluene.

the Soret band at 421 nm. The absorbance of the porphyrin thin film on glass in the early stage of the reaction showed the absorption maximum similar to that in toluene, while it was shifted to 434 nm in the end. This implies that the local density of porphyrins increases as the reaction progressed so that the intermolecular interactions between porphyrin chromophores cause exciton coupling, resulting in broadening and the red shift of the Soret band.

Determination of amounts of porphyrins bound to silicate glass

The amounts of porphyrin bonded to silicate glass was determined by hydrolysis of silicate ester linkage under basic conditions, followed by the UV-visible spectroscopic determination of the quantities of the hydrolysed porphyrin. While acid catalysed hydrolysis of the silicate ester linkage always gave some porphyrins remained on silicate glass, hydrolysis under basic conditions proceeded completely.¹⁰ The porphyrin bonded silicate glass was subjected to alkaline hydrolysis by immersing it in 0.1 M NaOH for 30 min at 50 °C. The hydrolysed porphyrin was collected in 6 mL of toluene and the concentration, c , was determined by use of UV-visible spectroscopy. The amount of bonded porphyrin Γ was calculated by Γ [molecules cm^{-2}] = c [M] \times 6 mL \times N_A/SA [cm^2], where N_A is the Avogadro number, SA is the surface area of the silicate glass. UV-visible spectra of the silicate glass after alkaline hydrolysis indicated that no porphyrin remained on the glass. The amounts of porphyrin bonded on silicate glass are listed in Table 1. Porphyrins carrying no long alkyl chains **1** and **5** showed the value of Γ of $18\text{--}20 \times 10^{13}$ molecules/ cm^2 , while porphyrin carrying long alkyl chains showed a much smaller value of Γ . Thus, steric bulk of alkyl chains would reduce the amount of adsorption. For the thiol derivatised porphyrins on gold, the amounts of porphyrin were reported to be in the range 1 to 17×10^{13} molecules/ cm^2 .¹³ The values listed in Table 1 are thus similar to those of the thiol derivatised porphyrin on gold.

Absorbances at the Soret band of porphyrin **1** on silicate glass are plotted against the amounts of bound porphyrins in Figure 2. There is a linear correlation, so that the absorbances of the Soret band of the UV-visible spectra of thin film on silicate glass can be used to evaluate the amounts of bound porphyrins. The rate constants of the adsorption reactions were determined by following the absorbance of the Soret band of porphyrin on the silicate glass as a function of time.

Table 1. The amounts of porphyrins **1**, **5** and **7** bound on silicate glass (Γ), and the absorption maxima (λ_{max}) and molar absorption coefficients (ϵ_{max}) in toluene.

	$\Gamma \times 10^{-13}$ /molecules cm^2	λ_{max} /nm	ϵ_{max} / $\text{cm}^{-1}\text{M}^{-1}$
Primary alcohol 1	18	421	4.38×10^5
cis-Diol 5	20	422	4.34×10^5
Alkyl cis-diol 7	11	426	5.35×10^5

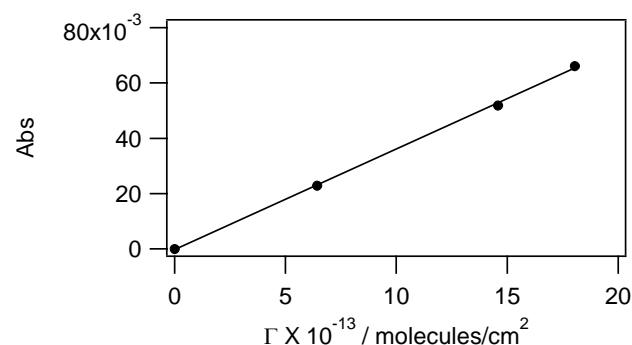


Fig. 2 Absorbance at the Soret band of UV-visible spectra of porphyrin **1** on silicate glass versus the amount of adsorbed porphyrin Γ determined by desorption experiments with alkaline hydrolysis. Linear regression analysis gave $\text{Abs} = 3.62 \times 10^{-16} \Gamma$, $R^2 = 0.9995$.

Reactivity of primary alcohol **1** and tertiary alcohol **2** with silicate glass

Figure 3 shows the plots of absorbance at the Soret band of **1** against the reaction time. We performed three independent runs to check the reproducibility of the kinetic data. The reaction with silicate glass proceeded fast for the initial 1 h, followed by the slower reaction, to reach a plateau, in which the absorbance of the Soret band was *ca.* 0.06. This absorbance at the plateau was almost constant for the heating temperatures of 160, 180, and 200 °C (data for 180 and 200 °C not shown).

When the progress of reaction of primary alcohol **1** and tertiary alcohol **2** with silicate glass are compared (see Figures 3 and 4), $\text{Abs}(t = 10 \text{ min})/\text{Abs}(t = \infty)$ of primary alcohol **1** was 0.65 at 160 °C, while that of tertiary alcohol **2** was 0.14. The reaction of tertiary alcohol was slower than that of primary alcohol and a

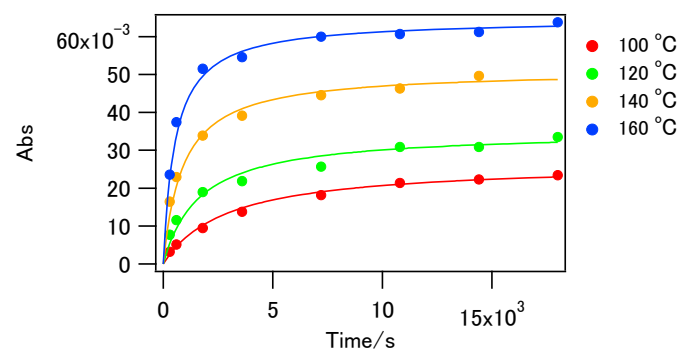


Fig. 3 Reaction of primary alcohol **1** with silicate glass. Lines calculated based on the pseudo-second order equation are shown.

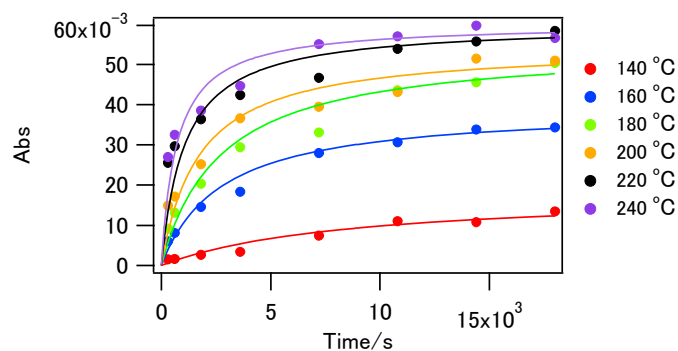


Fig. 4 Reaction of tertiary alcohol **2** with silicate glass. Lines calculated based on the pseudo-second order equation are shown.

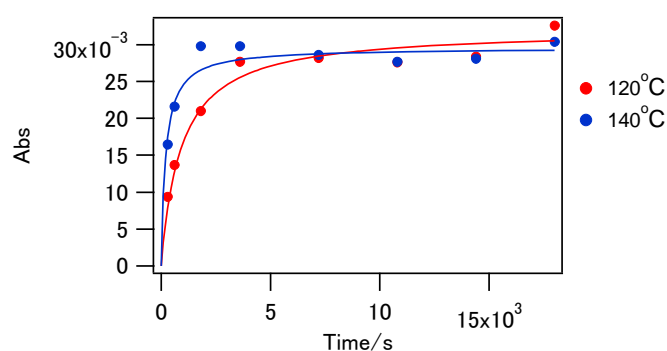


Fig. 5 Reaction of benzyl alcohol porphyrin **3** with silicate glass. Lines calculated based on the pseudo-second order equation are shown.

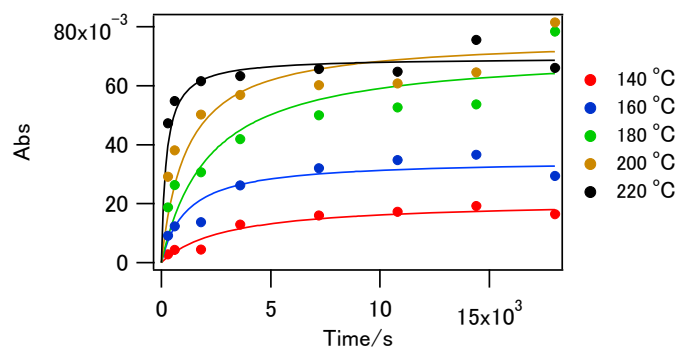


Fig. 6 Reaction of bromide porphyrin **4** with silicate glass. Lines calculated based on the pseudo-second order equation are shown.

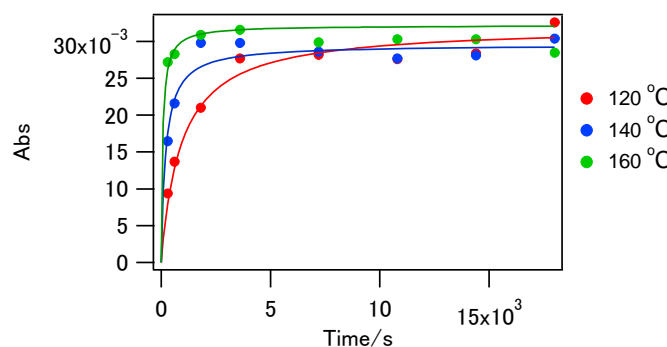


Fig. 7 Reaction of alkyl benzyl alcohol **6** with silicate glass. Lines calculated based on the pseudo-second order equation are shown.

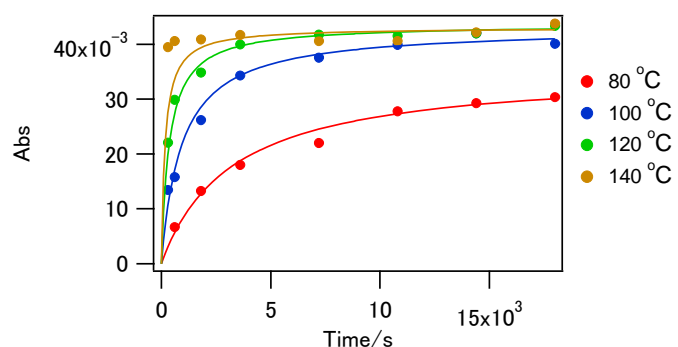


Fig. 8 Reaction of alkyl cis-diol porphyrin **7** with silicate glass. Lines calculated based on the pseudo-second order equation are shown.

higher reaction temperature was necessary for tertiary alcohol to form a monolayer. It should be noted that the saturated absorbance $Abs(t = \infty)$ of **2** was almost the same as that of **1**. Therefore, both **1** and **2** formed a densely packed monolayer film.

Effects of the spacer between the OH group and the porphyrin framework on the reactivity

Figure 5 shows the progress of reactions of benzyl alcohol appended porphyrin **3** with silicate glass. The extent of the reaction, $Abs(t = 60 \text{ min})/Abs(t = \infty)$, of **3** was almost 100% at 140 °C, while that of **1** was only 60%. However, it should be noted that the saturated absorbance of porphyrin **3** was only 0.03,

smaller than that of porphyrin **1**. Therefore **3** forms a loosely packed monolayer. The flexible spacer group between the hydroxy group and the rigid porphyrin framework seemed necessary to form a dense monolayer of porphyrin.

Comparison of reactivity of alcohols and bromides with silicate glass and effects of alkyl chains on the reactivity

Figure 6 shows the plots of absorbance of bromide porphyrin **4** as a function of time. Reaction of bromide porphyrin **4** was slow, and heating above 180 °C was necessary to obtain the similar absorbance as that of **1**. Figures 7 and 8 show the plots of absorbance of alkyl porphyrins **6** and **7**. These alkyl porphyrins **6** and **7** reacted rapidly, and plateau was reached when heated at 120 °C for 2 h.

Rate constants obtained from pseudo-second order equation

Kinetics of adsorption of porphyrins on silicate surface was previously analysed¹⁴ based on the pseudo-first order equation, i.e., the Lagergren equation:¹⁵

$$\ln(\Gamma_0 - \Gamma(t)) = \ln(\Gamma_0) - k_1 t. \quad (1)$$

where Γ_0 is the amounts of porphyrin adsorbed after plateau was reached, $\Gamma(t)$ is the amount of adsorbed porphyrin at time t , and k_1 is the pseudo-first order rate constant. The plot of $\ln(1 - \Gamma(t)/\Gamma_0)$ against t , however, gave a linear line with non-zero intercept in most cases. We found that the data were better fitted to the pseudo-second order equation:^{16,17}

$$\frac{t}{\Gamma(t)} = \frac{1}{k\Gamma_0^2} + \frac{1}{\Gamma_0} t \quad (2)$$

where t is the reaction time (s), k is the pseudo-second order rate constant ($\text{molecules}^{-1} \text{cm}^2 \text{s}^{-1}$), $\Gamma(t)$ is the amount of adsorbed porphyrin at time t ($\text{molecules}/\text{cm}^2$), and Γ_0 is the saturated amount of adsorbed porphyrin. There are a number of studies employing the pseudo-second order equation for kinetic analysis of adsorption of organic molecules and metal ions on solid surface.¹⁸ Linear regression analysis of the plot of $t/\Gamma(t)$ against t yielded the rate constant k (Table 2). At 140 °C, the rate constants decreases in the order: alkylporphyrins **6** and **7** > primary alcohols **1** ~ **3** > bromide **4** > tertiary alcohol **2**.

The Arrhenius plots of $\ln k$ against $1/T$ for the reaction of porphyrins **1**–**4** and **6** with silicate glass are shown in Figure 9. The activation energy E_a and the frequency factor A were determined based on the equation: $\ln k = -E_a/RT + \ln A$, and are listed in Table 3.

Table 2. Pseudo-second order rate constants of reaction of porphyrins with silicate glass.

	Temperature, °C	$k/\text{molecules}^{-1} \text{cm}^2 \text{s}^{-1}$
Primary alcohol 1	100	$(4.6 \pm 0.4) \times 10^{-18}$
	120	$(6 \pm 1) \times 10^{-18}$
	140	$(8 \pm 1) \times 10^{-18}$
	160	$(1.02 \pm 0.09) \times 10^{-17}$
Tertiary alcohol 2	180	$(2.5 \pm 0.7) \times 10^{-18}$
	200	$(3.9 \pm 1.0) \times 10^{-18}$
	220	$(6 \pm 2) \times 10^{-18}$
	240	$(9 \pm 2) \times 10^{-18}$
Benzyl alcohol 3	140	$(8 \pm 2) \times 10^{-18}$
	160	$(8 \pm 2) \times 10^{-18}$
	180	$(1.2 \pm 0.4) \times 10^{-17}$
Bromide 4	180	$(6 \pm 2) \times 10^{-18}$
	200	$(1.1 \pm 0.4) \times 10^{-18}$
Alkyl benzyl alcohol 6	220	$(2 \pm 1) \times 10^{-17}$
	120	$(1.2 \pm 0.5) \times 10^{-17}$
	140	$(6 \pm 3) \times 10^{-17}$
Alkyl cis-diol 7	160	$(1.6 \pm 0.2) \times 10^{-16}$
	80	$(3.2 \pm 0.4) \times 10^{-18}$
	100	$(9 \pm 2) \times 10^{-18}$
	120	$(2.3 \pm 0.6) \times 10^{-17}$
	140	$(5 \pm 4) \times 10^{-17}$

Activation energies of the reaction of gaseous methanol, ethanol, 1-propanol, and 1-butanol with silica gel were reported to be in the range of 29–46 kJ/mol.¹⁹ The activation energies listed in Table 3 are scattered in the range 15–105 kJ/mol: solid-solid reaction should be much complex than gas-solid reactions, because molecular motion to reach the transition state could be much restricted in the solid state.

When porphyrins **1** and **2** were compared, the slower reaction of **2** with silicate glass was ascribed to the larger activation energy. The slower reaction of bromide **4** also originated from the larger activation energy. Because bromide **4** is primary, one can assume that the reaction proceeds by a nucleophilic attack of a silanol group at the primary carbon through the S_N2 mechanism. On the other hand, the reaction of alcohols with silicate glass can proceed through the attack of alcohol oxygen on Si, followed by elimination of water.²⁰ Although there is discussion whether the reaction proceeds through the addition-elimination mechanism or the five-coordinated transition state,²⁰ the different mechanism between alcohol and bromide would lead to the

difference in the activation energy of the reaction. The reaction rate of porphyrin **3** with silicate glass was similar to that of porphyrin **1**, and the values of activation energy and the frequency factor were similar.

For the effects of alkyl chains on the reaction rates, the higher rate of reaction of alkyl porphyrins **6** and **7** than that of **1** was ascribed to the larger frequency factor. The reactions were performed above the melting point of **6**, so that **6** was in a liquid state during the reaction. The reaction temperatures of 80–120 °C were lower than the melting point of **7**, so that **7** was in the solid state during the reaction. Due to flexible long alkyl chains of **6** and **7**, the reorientation of the porphyrin can be facilitated to result in higher reactivity of alkyl porphyrins.

The rate constants of **1**, **2**, **3**, **4**, **6**, and **7** with silicate glass at 180 °C, calculated using these kinetic parameters, were 13, 2, 11, 2, 510, and $220 \times 10^{-18} \text{ molecules}^{-1} \text{cm}^2 \text{s}^{-1}$, respectively, showing that there is two-orders of magnitude acceleration by changing the molecular structures of the porphyrin. In particular, introduction of dodecyl groups to hydroxyporphyrin **3** accelerated the anchoring reaction by a factor of 50.

Table 3. Kinetic parameters for the reaction of porphyrins with silicate glass

	$E_a/\text{kJ mol}^{-1}$	$\ln(A/\text{molecules}^{-1} \text{cm}^2 \text{s}^{-1})$
Primary alcohol 1	17.4 ± 0.4	-34.3 ± 0.1
Tertiary alcohol 2	39.8 ± 0.8	-29.9 ± 0.2
Benzyl alcohol 3	15 ± 9	-35 ± 3
Bromide 4	105 ± 30	-13 ± 8
Alkyl benzyl alcohol 6	91 ± 9	-11 ± 3
Alkyl cis-diol 7	56 ± 1	-21.3 ± 0.3

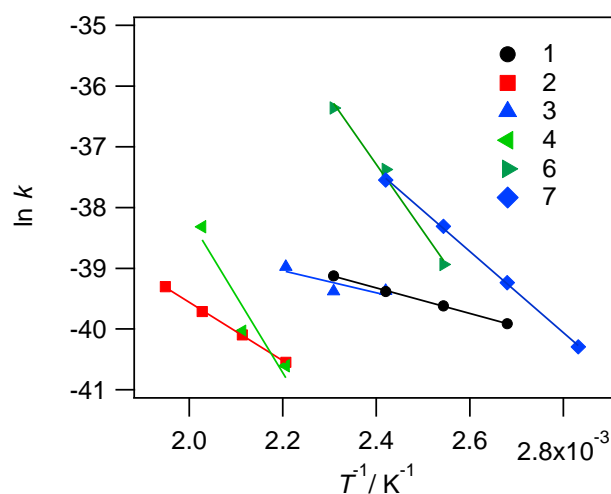


Fig. 9 Arrhenius plots of the reaction of various porphyrins **1**–**4**, **6**–**7** with silicate glass.

Conclusion

Porphyrins bearing either OH or Br as an anchoring group was reacted with silicate glass. The reactivity of porphyrin was high for primary alcohol with flexible linker between the OH group and the porphyrin framework. Long alkyl chains on porphyrin lowered the melting points and improved the reactivity, even in the reaction performed above the melting points. Tertiary alcohol and bromoalkyl porphyrin were less reactive than primary alcohol. The kinetics of the reaction between porphyrin and silicate glass was analysed by the pseudo-second order equation.

Slower reactions of tertiary alcohol and primary bromide than primary alcohol were attributed to the higher activation energy. Faster reaction of primary alcohol with long alkyl chains originated from the larger frequency factor. Both the intrinsic reactivity of the molecule and the dynamics of the interface played important roles in the anchoring reaction.

Experimental Section

General information

UV–visible spectra were obtained with a Perkin-Elmer Lambda 950 spectrophotometer. Spin-coating on a silicate glass was performed using a Mikasa MS-A 100 spin-coater. A hot stage Mettler-Toledo FP82HT was used for heat treatment of the spin-coated film. A silicate glass was prepared by splitting Matunami 76 × 26 mm borosilicate slide glass almost evenly into three pieces. ¹H NMR spectra were recorded with a JEOL JNM-ECA500 spectrometer. Tetramethylsilane was used as an internal standard. Matrix-assisted laser desorption–ionization time-of-flight mass (MALDI-TOF MS) spectra were recorded on a Bruker Daltonics Autoflex Speed spectrometer. Elemental analysis was obtained from Centre for Organic Elemental Microanalysis of Kyoto University.

Porphyrim **3** was prepared according to the literature, and its ¹H NMR data were identical with those reported.²¹ Preparation of porphyrins **1**, **2**,¹⁰ **5** and **7**⁹ were reported previously.

Determination of the amounts of bound porphyrin on silicate glass

The porphyrin bonded silicate glass was subjected to alkaline hydrolysis by immersing it in 0.1 M NaOH for 30 min at 50 °C. The silicate glass was washed with distilled water and the washing was combined with the 0.1 M NaOH. The alkaline aqueous solution was neutralized with 0.1 M HCl, and the water was evaporated in vacuo. The residual NaCl salt was washed with toluene. The silicate glass was also washed with toluene. The toluene washing was combined with the washing of the NaCl salt, and messed up to 6 mL. The concentration of porphyrin, *c*, in toluene was determined by UV–visible spectroscopy.

5-(4-(5-Bromopentyloxy)phenyl)-10,15,20-triphenylporphyrin 4. 5-(4-(5-Hydroxypentyloxy)phenyl)-10,15,20-triphenylporphyrin **1**⁹ (100 mg, 0.139 mmol), CBr₄ (148 mg, 0.446 mmol), and triphenylphosphine (117 mg, 0.446 mmol) were placed in a 200-mL flask and purged with Ar. Dry CH₂Cl₂ (50 mL) was added and the mixture was stirred at room temperature for 4 h. The reaction mixture was washed with sat. NaHCO₃ aq. four times and then with water once. The CH₂Cl₂ solution was dried over anhydrous Na₂SO₄, and evaporated. The residue was subjected to SiO₂ column chromatography eluted with CHCl₃–hexane (3:2), to yield 92.4 mg (85%) of **4**.

¹H NMR (500 MHz, CDCl₃): δ (ppm) = –2.77 (s, 2H; NH), 1.82 (m, 2H; CH₂CH₂Br), 2.00–2.07 (m, 4H; Ph-OCH₂CH₂CH₂), 3.54 (m, 2H; CH₂Br), 4.26 (m, 2H; Ph-OCH₂), 7.27 (one of the doublet signals, the other was overlapped with CHCl₃, 2H; 5-phenylene H-3'), 7.75 (m, 9H; 10,15,20-phenyl H-3', H-4'), 8.11 (m, 2H; 5-phenylene H-2'), 8.21 (m, 6H; 10,15,20-phenyl H-2'), 8.84 (m, 6H; pyrrole-β-H), 8.88 (m, 2H; pyrrole-β-H); MS

(MALDI-TOF): *m/z* = 779 [M+H]⁺ (calcd. for C₄₉H₃₉BrN₄O *m/z* = 778). Elemental analysis: Found: C, 75.3; H, 5.2; N, 7.0, Br, 10.0. Calc. for C₄₉H₃₉BrN₄O: C, 75.5; H, 5.0; N, 7.2; Br, 10.25%.

5-(4-Carbomethoxyphenyl)-10,15,20-tris(3,4-didodecyloxyphenyl)porphyrin 10. 3,4-Didodecyloxybenzaldehyde²² (7.50 g, 15.8 mmol) and methyl 4-formylbenzoate (2.59 g, 15.8 mmol) were dissolved in propionic acid (200 mL). After the solution was heated to 160 °C, pyrrole (2.12 g, 31.6 mmol) was added. The reaction mixture was heated at 160 °C for 30 min. The propionic acid was then removed by vacuum distillation, and the residue was chromatographed on SiO₂ eluted with CHCl₃–hexane (3:2) to yield 499 mg (5.3 %) of **10**.

¹H NMR (500 MHz, CDCl₃): δ (ppm) = –2.77 (s, 2H; NH), 0.84 (t, *J* = 6.00 Hz, 9H; CH₃), 0.90 (t, *J* = 6.00 Hz, 9H; CH₃), 1.20–2.04 (m, 120H; –OCH₂(CH₂)₁₀CH₃), 4.11–4.13 (m, 9H; –OCH₂(CH₂)₁₀CH₃ and Ph-COOCH₃), 4.29 (m, 6H; –OCH₂(CH₂)₁₀CH₃), 7.23 (m, 3H; 10,15,20-phenylene H-5'), 7.70 (m, 3H; 10,15,20-phenylene H-6'), 7.77 (m, 3H; 10,15,20-phenylene H-2'), 8.30 (m, 2H; 5-phenylene H-3'), 8.43 (m, 2H; 5-phenylene H-2'), 8.76 (m, 2H; pyrrole-β-H), 8.91 (m, 6H; pyrrole-β-H); MS (MALDI-TOF): *m/z* = 1778 [M+H]⁺ (calcd. for C₁₁₈H₁₇₆N₄O₈ *m/z* = 1777).

5-(4-Hydroxymethylphenyl)-10,15,20-tris(3,4-didodecyloxyphenyl)porphyrin 6. LiAlH₄ (36.7 mg, 0.97 mmol) was placed in a 100-mL flask and the flask was purged with Ar. A solution of porphyrin **10** (215 mg, 0.121 mmol) in dry THF (50 mL) was then added via syringe. The reaction mixture was stirred for 1.5 h at room temperature. The excess of reagent was decomposed with Na₂SO₄·10H₂O. The mixture was filtered and the filtrate was evaporated. Column chromatography on SiO₂ eluted with CHCl₃–hexane (4:1) gave 159 mg (75 %) of **6**.

¹H NMR (500 MHz, CDCl₃): δ (ppm) = –2.76 (s, 2H; NH), 0.84 (t, *J* = 6.90 Hz, 9H; CH₃), 0.90 (t, *J* = 6.90 Hz, 9H; CH₃), 1.21–2.05 (m, 121H; –OCH₂(CH₂)₁₀CH₃ and –CH₂OH), 4.12 (m, 6H; –OCH₂(CH₂)₁₀CH₃), 4.28 (m, 6H; –OCH₂(CH₂)₁₀CH₃), 5.05 (s, 2H; –CH₂OH), 7.22 (m, 3H; 10,15,20-phenylene H-5'), 7.73 (m, 8H; 10,15,20-phenylene H-2', H-6' and 5-phenylene H-3'), 8.20 (s, 2H; 5-phenylene H-2'), 8.82 (m, 2H; pyrrole-β-H), 8.90 (m, 6H; pyrrole-β-H); MS (MALDI-TOF): *m/z* = 1750 [M+H]⁺ (calcd. for C₁₁₇H₁₇₆N₄O₇ *m/z* = 1749). Elemental analysis: Found: C, 80.1; H, 10.1; N, 3.2. Calc. for C₁₁₇H₁₇₆N₄O₇: C, 80.3; H, 10.1; N, 3.2%.

Acknowledgements

This work was supported by "Creating Research Centre for Advanced Molecular Biochemistry", Strategic Development of Research Infrastructure for Private Universities, the Ministry of Education, Culture, Sports, Science and Technology (MEXT), Japan. This work was partially supported by a Grant-in-Aid for Scientific Research (C) (Grant number 23550165) from the Japan Society for the Promotion of Science.

Notes and references

^a Department of Molecular Chemistry and Biochemistry, Faculty of Science and Engineering, Doshisha University, Kyotanabe, Kyoto 610-0321 Japan.

- 1 (a) J. D. Swalen, D. L. Allara, J. D. Andrade, E. A. Chandross, S. Garoff, J. Israelachvili, T. J. McCarthy, R. Murray, R. F. Pease, J. F. Rabolt, K. J. Wynne, and H. Yu, *Langmuir*, 1987, **3**, 932; (b) Z. Ma and F. Zaera, *Surface Science Reports*, 2006, **61**, 229; (c) C. Nicosia and J. Huskens, *Mater. Horiz.*, 2014, **1**, 32; (d) S. Onclin, B. J. Ravoo, and D. N. Reinhoudt, *Angew. Chem. Int. Ed.*, 2005, **44**, 6282; (e) S. A. Claridge, W.-S. Liao, J. C. Thomas, Y. Zhao, H. H. Cao, S. Cheunkar, A. C. Serino, A. M. Andrews, and P. S. Weiss, *Chem. Soc. Rev.*, 2013, **42**, 2725.
- 2 Y. Yin and A. P. Alivisatos, *Nature*, 2005, **437**, 664.
- 3 Q. Gao, S. Wang, Y. Tang, and C. Giordano, *Chem. Commun.*, 2012, **48**, 260.
- 4 L. Feng, L. Jing, and Z. Shusheng, *Talanta*, 2008, **74**, 1247.
- 5 (a) A. Gulino, P. Mineo, S. Bazzano, D. Vitalini, and I. Fragala, *Chem. Mater.*, 2005, **17**, 4043; (b) S. Xie, S. Bao, J. Ouyang, X. Zhou, Q. Kuang, Z. Xie, and L. Zheng, *Chem. Eur. J.*, 2014, **20**, 5244.
- 6 (a) A. Ulman, *Chem. Rev.*, 1996, **96**, 1533; (b) L. H. Dubois and R. G. Nuzzo, *Annu. Rev. Phys. Chem.*, 1992, **43**, 437; (c) J. C. Love, L. A. Estroff, J. K. Kriebel, R. G. Nuzzo, and G. M. Whitesides, *Chem. Rev.*, 2005, **105**, 1103.
- 7 (a) L. Wei, D. Syomin, R. S. Loewe, J. S. Lindsey, F. Zaera, and D. F. Bocian, *J. Phys. Chem. B*, 2005, **109**, 6323; (b) M. A. Khaderbad, A. Kushagra, M. Ravikanth, and V. R. Rao, in "'Bottom-up" approaches for nanoelectronics', ed. D. Vasileska, InTech, Rijeka, Croatia, 2010; (c) Muthukumar, P.; John, S. A. *Electrochimica Acta* 2014, **115**, 197-205.
- 8 (a) C. C. Ballard, E. C. Broge, R. K. Iler, D. S. S. John, and J. R. McWhorter, *J. Phys. Chem.*, 1961, **65**, 20; (b) G. C. Ossenkamp, T. Kemmitt, and J. H. Johnston, *Chem. Mater.*, 2001, **13**, 3975; (c) G. C. Ossenkamp, T. Kemmitt, and J. H. Johnston, *Langmuir*, 2002, **18**, 5749.
- 9 N. Furuta and T. Mizutani, *Thin Solid Films*, 2014, **556**, 174.
- 10 N. Furuta, T. Yagi, and T. Mizutani, *Tetrahedron*, 2014, **70**, 4336.
- 11 J. Martensson, K. Sandros, and O. Wennerstroem, *Tetrahedron Lett.*, 1993, **34**, 541.
- 12 E. Sun, X. Cheng, D. Wang, C. Zhuang, A. Xia, and T. Shi, *J. Coord. Chem.*, 2009, **62**, 1584.
- 13 (a) K. Shimazu, M. Takechi, H. Fujii, M. Suzuki, M. Suzuki, H. Saiki, T. Yoshimura, and K. Uosaki, *Thin Solid Films*, 1996, **273**, 250; (b) A. L. Bramblett, M. S. Boeckl, K. D. Hauch, B. D. Ratner, T. Sasaki, and J. W. R. Jr., *Surf. Interface Anal.*, 2002, **33**, 506.
- 14 N. Minamijima, N. Furuta, S. Wakunami, and T. Mizutani, *Bull. Chem. Soc. Jpn.*, 2011, **84**, 794.
- 15 (a) S. Lagergren, *Kungliga Svenska Vetenskapsakademiens Handlingar*, 1898, **24**, 1; (b) W. Rudzinski and W. Plazinski, *J. Phys. Chem. C*, 2007, **111**, 15100.
- 16 (a) Y. S. Ho and G. McKay, *Process Biochemistry*, 2003, **38**, 1047. (b) Y. S. Ho and G. McKay, *Wat. Res.*, 2000, **34**, 735.
- 17 (a) V. C. Srivastava, M. M. Swamy, I. D. Mall, B. Prasad, and I. M. Mishra, *Colloids and Surfaces A: Physicochem. Eng. Aspects*, 2006, **272**, 89; (b) S. S. Gupta and K. G. Bhattacharyya, *J. Colloid Interface Sci.*, 2006, **295**, 21; (c) K. V. Kumar, *J. Hazardous Materials*, 2007, **142**, 564; (d) K. D. Belaid, S. Kacha, M. Kameche, and Z. Derriche, *J. Environmental Chem. Eng.*, 2013, **1**, 496.
- 18 B. Boe, *J. Organometallic Chem.*, 1976, **107**, 139.
- 19 S. Shioji, M. Kawaguchi, Y. Hayashi, K. Tokami, and H. Yamamoto, *Advanced Powder Technology*, 2001, **12**, 343.
- 20 (a) H. Schmidt, H. Scholze, and A. Kaiser, *J. Non-Crystalline Solids*, 1984, **63**, 1; (b) C. J. Brinker, *J. Non-Crystalline Solids*, 1988, **100**, 31.
- 21 G. Liu, A. N. Khlobystov, G. Charalambidis, A. G. Coutsolelos, G. A. D. Briggs, and K. Porfyrakis, *J. Am. Chem. Soc.*, 2012, **134**, 1938.
- 22 R. Murakami, A. Minami, and T. Mizutani, *Org. Biomol. Chem.*, 2009, **7**, 1437.